FINITE ELEMENT ANALYSIS OF STRESSES IN FUEL ELEMENTS OF A HIGH-TEMPERATURE GAS-COOLED REACTOR

J.L. HEAD, A. JEZERNIK,

Nuclear Power Section, Department of Mechanical Engineering, Imperial College of Science and Technology, London, United Kingdom

ABSTRACT

A computer programme is described, written to analyse the time-dependent stresses in prismatic fuel elements of a High-temperature Gas-cooled Reactor. Results are given of an analysis of the stress history of a teledial fuel pin throughout the life of the fuel pin in a reactor.

1. INTRODUCTION

One form of fuel element which is being considered for use in the High-temperature Gas-cooled Reactor (HTR) consists of a prismatic block of graphite containing an array of axial channels in which fuel pins are located and along which the coolant (helium) flows. Several types of fuel pin are being considered, including the hollow rod, the tubular fuel pin and the so-called teledial pin. Detailed descriptions of these fuel pins are given by Head and Kinkead [1] in a complementary paper which reviews the thermal and stress analysis problems associated with the fuel pins and the multi-channel graphite blocks.

The temperature and stress distributions in the hollow rod and tubular fuel pins may be analysed by one-dimensional methods, at least in regions away from the ends of the pin and provided that the neutron flux and temperature distributions are axi-symmetric. The teledial fuel pin and the multi-channel blocks require two-dimensional analyses. This paper describes a two-dimensional finite element computer programme which has been developed for this purpose by Jezernik [2]. Results are included of an analysis of the stress history of a teledial fuel pin throughout its life in a reactor.

The effects of fast neutron irradiation of graphite have been described in detail elsewhere (see for example Nightingale [3] and Simmons [4]); only the briefest account is included here. Collisions between neutrons and carbon atoms result in the displacement of carbon atoms from lattice positions, the displaced atoms generally having sufficient energy to cause further displacements. Point defects of the crystal lattice are thus created, which cause dimensional changes of polycrystalline graphite and changes of many of the physical and mechanical properties, including thermal conductivity, thermal expansion coefficient, elastic moduli and strength. The numbers of point defects created, and the subsequent behaviour of the defects, which together determine the dimensional and property changes, depend respectively on the neutron dose and energy spectrum• and on the graphite temperature.

In the fuel pins, gradients of temperature lead to spatial variations of the irradiation - induced dimensional changes••, which, combined with differential thermal strains, generate stresses in the pin. In the multi-channel blocks there are also significant variations of neutron energy spectrum which also lead to variation of the dimensional changes and are therefore a source of stress. The stresses are modified by irradiation-activated creep of the graphite. If a graphite specimen is irradiated under stress, transient and steady creep are observed. The transient creep rate reduces rapidly with increasing neutron dose, the total transient creep strain being approximately equal to the elastic strain. The steady creep rate is independent of neutron dose, is directly proportional to the applied stress and depends strongly on the graphite temperature.

Previous work in this field includes two-dimensional analyses of the stresses in multi-channel graphite blocks by Witt and Greenstreet [6] and by Chang and Rashid [7]. Witt and Greenstreet used a finite difference method and assumed elastic response of the graphite. Chang and Rashid used a finite element method, assuming an appropriate viscoelastic model and using an hereditary integral form of the constitutive equation.

••The irradiation-induced dimensional changes are sometimes termed "Wigner strains".

•An allowance may be made for the dependence on energy spectrum by use of an "equivalent dose", a concept introduced by Bell et al. [5]. In the work described in the paper, the DIDO equivalent dose is used.

The method of analysis described in this paper is an extension of the method proposed by Mendelson et al. [8] and widely used in the solution of problems of thermal creep. The basis of the method is the separation of the strain tensor into elastic strain, thermal strain, irradiation and creep strain tensors which are calculated separately. The solution is advanced by time steps and at the end of each step the stresses are obtained by a linear-elastic finite element analysis, which makes allowance for thermal strains, Wigner strains and creep strains, the creep strains being obtained by summation of the incremental creep strains over all previous time intervals. At the end of each time step, the temperature distribution may be re-calculated, making allowance for changes of heat flux and graphite conductivity. Other graphite properties which depend on temperature and neutron dose may be adjusted before advancing the calculation by a further time step.

2. THEORY

The theory is here outlined in symbolic form, some of the matrices being developed in the Appendix.

The analysis uses triangular elements with a linear displacement field defined by:

$$\begin{aligned} u &= u_i + C_1 (x - x_i) + C_2 (y - y_i) \\ v &= v_i + C_3 (x - x_i) + C_4 (y - y_i) \end{aligned} \qquad (1)$$

The derivation of the force/displacement relationship of the element is well known and is not repeated. The relationship is derived in the following form by Wilson [9]:

$$\{s\} = [k]\{\delta\} \qquad (2)$$

where the element stiffness matrix $[k]$ is given by:

$$[k] = \Delta [B]^T [D][B] \qquad (3)$$

The force/displacement matrix for the complete assembly of elements is given by:

$$\{R\} = [K]\{r\} \qquad (4)$$

Where $[K]$, the stiffness matrix for the complete assembly, is formed by superposition of the element stiffness matrices. The nodal point displacements are given by:

$$\{r\} = [K]^{-1}\{R\} \qquad (5)$$

The element stresses, in the xy plane, which are necessary to suppress the combined thermal, Wigner and creep strains are given by:

$$\{\sigma^*\} = -[D]\left\{\{\varepsilon^t\} + \{\varepsilon^W\} + \{\varepsilon^C\}\right\} \tag{6}$$

The element corner forces to maintain these stresses are determined by pre-multiplying $\{\sigma^*\}$ by $\Delta[B]^T$. Thus the nodal forces $\{R^*\}$ to suppress the combined thermal, Wigner and creep strains are obtained. The complete assembly is then analysed assuming nodal forces $\{R\} - \{R^*\}$ and the element stresses obtained by adding the stresses due to these nodal forces to the stresses given by eq. (6).

The axial stress on the nth element, necessary to suppress the strain in the axial (z) direction, is:

$$(\sigma_z)_n = \nu_{//}(\sigma_x + \sigma_y)_n - E_{//}(\varepsilon_z{}^t + \varepsilon_z{}^W + \varepsilon_z{}^C)_n \tag{7}$$

The total restraining force in the axial direction is given by:

$$P = \sum_n \left\{\left[\nu_{//}(\sigma_x + \sigma_y)_n - E_{//}(\varepsilon_z{}^t + \varepsilon_z{}^W + \varepsilon_z{}^C)_n\right] A_n\right\} \tag{8}$$

In the present analysis, it is assumed that the fuel pin is free of axial restraint, the axial stress on the nth element is given therefore by:

$$(\sigma_z)_n = -\frac{1}{A}_{\text{total}} \sum_n \left\{\left[\nu_{//}(\sigma_x + \sigma_y)_n - E_{//}(\varepsilon_z{}^t + \varepsilon_z{}^W + \varepsilon_z{}^C)_n\right] A_n\right\}$$

$$+ \nu_{//}(\sigma_x + \sigma_y)_n - E_{//}(\varepsilon_z{}^t + \varepsilon_z{}^W + \varepsilon_z{}^C)_n \tag{9}$$

3. COMPUTER PROGRAMME

The determination of the nodal point displacements, hence the element strains and stresses, requires the solution of the system of equations:

$$\{r\} = [K]^{-1}\left\{\{R\} - \{R^*\}\right\} \tag{10}$$

The methods commonly used for the solution of such systems of equations may be divided into two categories, direct methods using Gaussian elimination, and iterative methods using a modified Gauss-Seidel technique. Two versions of the programme have been developed for the London University CDC 6600 computer, one using a direct (band) method, the other using the iterative method. Preliminary work indicated that for the present analysis, using triangular elements with a linear displacement field, with 605 elements and 379 nodes, the iterative method

was faster. For analyses using more complex elements, or for analyses using larger numbers of elements, a direct method may well be more suitable.

The results given in this paper were therefore obtained using the iterative programme, for which a simplified flow diagram is included as fig. 1. The computer time used for this analysis was approximately twenty minutes.

4. ANALYSIS OF TELEDIAL FUEL PIN

Fig. 2 shows a sector of the teledial fuel pin, bounded by planes of symmetry. The fig. also shows the mesh used in the analysis. The assumed temperature distribution, shown in fig. 3, was provided by Kinkead [10] and corresponds to the time in the life of the fuel pin when the maximum fuel temperature occurs. This temperature distribution was assumed to remain unchanged throughout the life of the fuel pin, although the programme permits the element temperatures to be re-read as frequently as required.

It was assumed that the fuel pin was made from a pressed Gilsocarbon graphite. The dimensional changes and other graphite data used in the analysis were assembled by Manzel [11] and by Everett et al. [12]. The equivalent neutron flux was assumed to be uniform over the cross-section of the fuel pin and the analysis continued to a DIDO equivalent Ni dose of 4×10^{21} n/cm^2, by 40 time intervals corresponding to equal dose increments of 1×10^{20} n/cm^2.

The initial (thermal) stresses are shown in figs. 4, 5 and 6. Figs. 7, 8 and 9 show the variation with time of the stresses on highly stressed elements in different regions of the fuel pin cross-section. These figs. (7, 8 and 9) show the stresses on these elements with the fuel pin at the operating temperature and also the residual stresses assuming that the fuel pin is allowed to cool to a uniform temperature of 20°C.

5. DISCUSSION OF RESULTS

As fig. 3 shows, the highest graphite temperature occurs in the ligaments between the fuel holes. With the particular boundary conditions used in the thermal analysis, the region inside the fuel hole pitch circle is generally hotter than the outer region. The lowest graphite temperature occurs in the rib, which locates the fuel pin in the channel.

The high temperature in the ligaments causes a moderately high compressive radial stress initially in these regions (see fig. 5). The high temperature generally, inside the fuel hole pitch circle, causes compressive stress in this region, which is concentrated around the edge of the fuel hole. It is in this region (element 488) that the highest stress in the xy plane occurs. Outside the fuel hole pitch circle, the stresses in the xy plane are tensile (see fig. 4) with a concentration in the corner of the rib. (The mesh used is too coarse to give a true indication of the peak stress). As fig. 6 shows, there is a very high axial tensile stress in the rib.

Fig. 7 shows the way in which the stresses on element 488 vary with time. The high compressive stress rapidly reduces in magnitude due to the combined effects of creep and a high irradiation shrinkage rate of the graphite (the shrinkage rate generally increases with increasing temperature). Towards the end of the life of the fuel pin, tensile stresses develop in this region due to the high shrinkage rate. Shut-down of the reactor at this time causes a high residual tensile stress.

Fig. 8 shows a similar variation with time of the stresses on element 401, which is in the ligament region. Fig. 9 shows the variation with time of the axial stress on element 4, which is in the rib. The stresses in the xy plane on this element are very low and have not been plotted. The fig. shows the rapid reduction of the initial tensile stress and development of a compressive stress due to the low shrinkage rate of the graphite in this (cool) region. The residual stress in the rib is high, but is compressive.

A general comment that may be made is that the calculated stresses, particularly the residual stresses which occur at the end of the fuel pin life, are almost certainly an over-estimate of the true stresses, as the reduction of pin power, due to burnup, has been neglected.

6. REFERENCES

[1] HEAD, J. L., KINKEAD, A. N., "Graphite Fuel Element Structures for High-temperature Gas-cooled Reactors", Paper to be presented at this Conference.

[2] JEZERNIK, A., "The Finite Element Analysis of Irradiation Induced Stresses in Graphite Core Components of a Nuclear Reactor". Thesis to be published, University of London.

[3] Nightingale, R. E., (Editor), "Nuclear Graphite", Academic Press, New York (1962).

[4] SIMMONS, J. H. W., "Radiation Damage in Graphite", Pergamon Press, Oxford (1965).

[5] BELL, J. C., BRIDGE, H., COTTRELL, A. H., GREENOUGH, G. B., REYNOLDS, W. N., SIMMONS, J. H. W., "Stored Energy in the Graphite of Power-Producing Nuclear Reactors", Phil. Trans. Roy. Soc. (A), 254, 361 (1962).

[6] WITT, F. J., GREENSTREET, B. L., "Influence of Cross-sectional Shape on Irradiation-induced Stresses in Graphite Columns", Nucl. Sci. and Engg., 25, 141 (1966).

[7] CHANG, T. Y., RASHID, Y. R., "Viscoelastic Response of Graphitic Materials in Irradiation Environments", Nucl. Engg. and Design, 14, 181 (1970).

[8] MENDELSON, A., HIRSCHBERG, M. H. MANSON, S. S., "A General Approach to the Practical Solution of Creep Problems", J. Basic Engg.,Trans. A.S.M.E., 81D, 585 (1959).

[9] WILSON, E. L., "Finite Element Analysis of Two-dimensional Structures" Thesis, University of California (1963).

[10] KINKEAD, A. N., private communication.

[11] MANZEL, R., private communication.

[12] EVERETT, M. R., BLACKSTONE, R., GRAHAM, L. W., MANZEL, R., "Graphite Materials Data for High Temperature Nuclear Reactors", Dragon Project Report 699 (1969).

7. NOTATION

	A	Area of element
	$[B]$	Displacement/strain transformation matrix
	$C_{1,2,3,4}$	Constants
	$[D]$	Elasticity matrix
	D_e	Equivalent neutron dose
	E	Young's modulus
	$[K]$	Stiffness matrix for complete assembly
	$[k]$	Stiffness matrix for element
	$m^2 = \frac{E_\perp}{E_{//}}$	
	P	Axial restraining force
	$[q]$	Creep compliance matrix
	$\{R\}$	Nodal force matrix
	$\{R^\bullet\}$	Nodal forces to suppress displacements
	$\{r\}$	Nodal displacement matrix
	$\{S\}$	Deviatoric stress matrix
	$\{s\}$	Element corner force matrix
	T	Temperature
	u,v	Element displacements in xy plane
	α	Thermal expansion coefficient
	$\{\delta\}$	Element corner displacement matrix
	$\{\varepsilon^e\}$	Elastic strain matrix
	$\{\varepsilon^c\}$	Creep strain matrix
	$\{\varepsilon^t\}$	Thermal strain matrix
	$\{\varepsilon^W\}$	Wigner strain matrix
	ν	Poisson's ratio
	$\{\sigma\}$	Stress matrix
	$\{\sigma^\bullet\}$	Stresses to suppress displacements
Subscripts	$\perp$	Perpendicular to extrusion or pressing direction
	$//$	Parallel to extrusion or pressing direction
	n	nth element

APPENDIX

DEVELOPMENT OF MATRICES

Elasticity Matrix

Nuclear graphite is manufactured either by extrusion or by pressing. Many of the physical and mechanical properties vary between the direction parallel to extrusion or pressing and the transverse direction. In the analysis, the z coordinate direction was assumed to coincide with the extrusion or pressing direction and the material was assumed to be isotropic in the transverse (xy) plane. The stress/strain relationship is then:

$$\begin{Bmatrix} \sigma_x \\ \sigma_y \\ \sigma_z \\ \tau_{xy} \end{Bmatrix} = [D] \begin{Bmatrix} \varepsilon_x^e \\ \varepsilon_y^e \\ \varepsilon_z^e \\ \gamma_{xy}^e \end{Bmatrix} \qquad (11)$$

Where

$$[D] = \frac{E}{(1+\nu_\perp)(1-\nu_\perp-2m^2\nu_{/\!/}^2)} \begin{bmatrix} 1-m^2\nu_{/\!/}^2 & \nu_\perp + m^2\nu_{/\!/}^2 & \nu_{/\!/}(1+\nu_\perp) & 0 \\ \nu_\perp + m^2\nu_{/\!/}^2 & 1-m^2\nu_{/\!/}^2 & \nu_{/\!/}(1+\nu_\perp) & 0 \\ \nu_{/\!/}(1+\nu_\perp) & \nu_{/\!/}(1+\nu_\perp) & \frac{1}{m^2}(1-\nu_\perp^2) & 0 \\ 0 & 0 & 0 & \frac{1}{2}(1-\nu_\perp-2m^2\nu_{/\!/}^2) \end{bmatrix} \qquad (12)$$

In plane strain ($\varepsilon_z = 0$) :

$$\sigma_z = \nu_{/\!/}(\sigma_x + \sigma_y) \qquad (13)$$

Thermal Strain Matrix

$$\{\varepsilon^t\} = \begin{Bmatrix} \varepsilon_x^t \\ \varepsilon_y^t \\ \varepsilon_z^t \\ \gamma_{xy}^t \end{Bmatrix} = \begin{Bmatrix} \alpha_\perp \\ \alpha_\perp \\ \alpha_{/\!/} \\ 0 \end{Bmatrix} T \qquad (14)$$

Wigner Strain Matrix

$$\{\varepsilon^W\} = \begin{Bmatrix} \varepsilon_x^W \\ \varepsilon_y^W \\ \varepsilon_z^W \\ \gamma_{xy}^W \end{Bmatrix} = \begin{Bmatrix} \varepsilon_\perp^W \\ \varepsilon_\perp^W \\ \varepsilon_{//}^W \\ 0 \end{Bmatrix} \tag{15}$$

Creep Strain Matrix

In the teledial analysis described in this paper, the transient creep was neglected and the (steady) creep strain rate matrix was assumed to be related to the deviatoric stress matrix by a relationship of the form:

$$\begin{Bmatrix} \dot{\varepsilon}_x^c \\ \dot{\varepsilon}_y^c \\ \dot{\varepsilon}_z^c \\ \dot{\gamma}_{xy}^c \end{Bmatrix} = \begin{bmatrix} q_{11} & q_{12} & q_{13} & 0 \\ q_{12} & q_{11} & q_{13} & 0 \\ q_{13} & q_{13} & q_{33} & 0 \\ 0 & 0 & 0 & 2(q_{11}-q_{12}) \end{bmatrix} \begin{Bmatrix} S_x \\ S_y \\ S_z \\ \tau_{xy} \end{Bmatrix} \tag{16}$$

where the dot indicates rate of change with respect to neutron dose. The creep compliances q_{11} and q_{33} have been measured experimentally, but not the compliances q_{12} and q_{13}. These were therefore expressed in terms of q_{11} and q_{33} by assuming that creep occurs at constant volume. (This assumption may not be valid for small strains, as the structure of graphite may permit some volume change, however, the assumption is probably increasingly valid for large strains). With this assumption, and multiplying both sides of eq. (16) by the incremental neutron dose received by the element, the incremental creep strains are given by:

$$\begin{Bmatrix} \delta\varepsilon_x^c \\ \delta\varepsilon_y^c \\ \delta\varepsilon_z^c \\ \delta\gamma_{xy}^c \end{Bmatrix} = \delta(D_e) \begin{bmatrix} q_{11} & -(q_{11}-\frac{1}{2}q_{33}) & -\frac{1}{2}q_{33} & 0 \\ -(q_{11}-\frac{1}{2}q_{33}) & q_{11} & -\frac{1}{2}q_{33} & 0 \\ -\frac{1}{2}q_{33} & -\frac{1}{2}q_{33} & q_{33} & 0 \\ 0 & 0 & 0 & 4q_{11}-q_{33} \end{bmatrix} \begin{Bmatrix} \sigma_x \\ \sigma_y \\ \sigma_z \\ \tau_{xy} \end{Bmatrix} \tag{17}$$

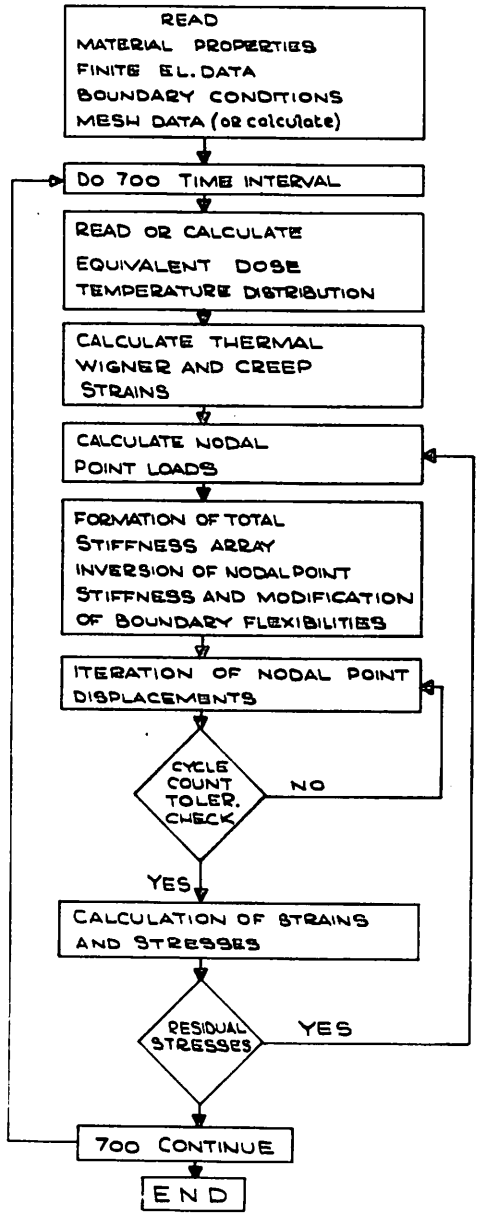

Fig. 1 Flow Diagram for Iterative Programme

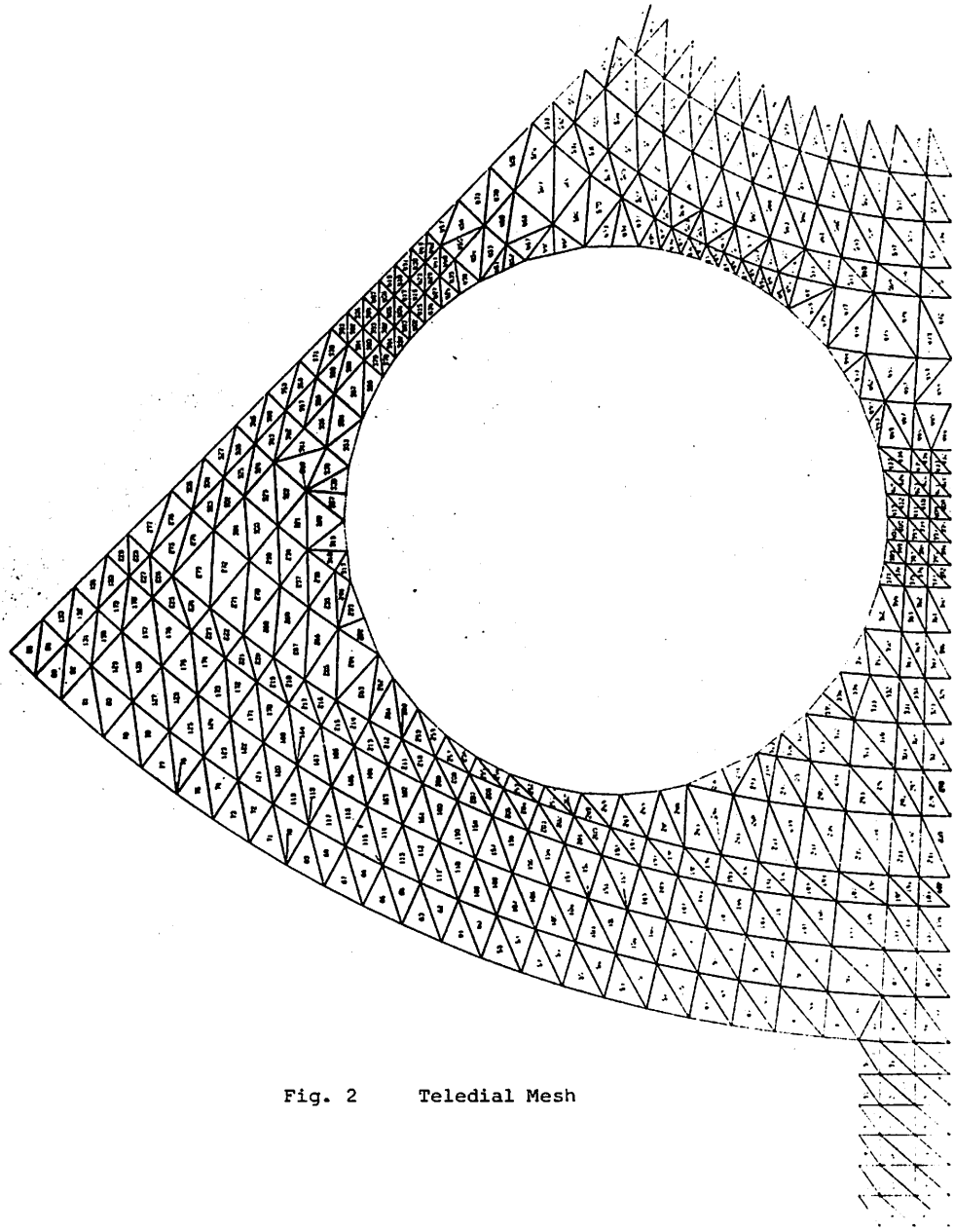

Fig. 2 Teledial Mesh

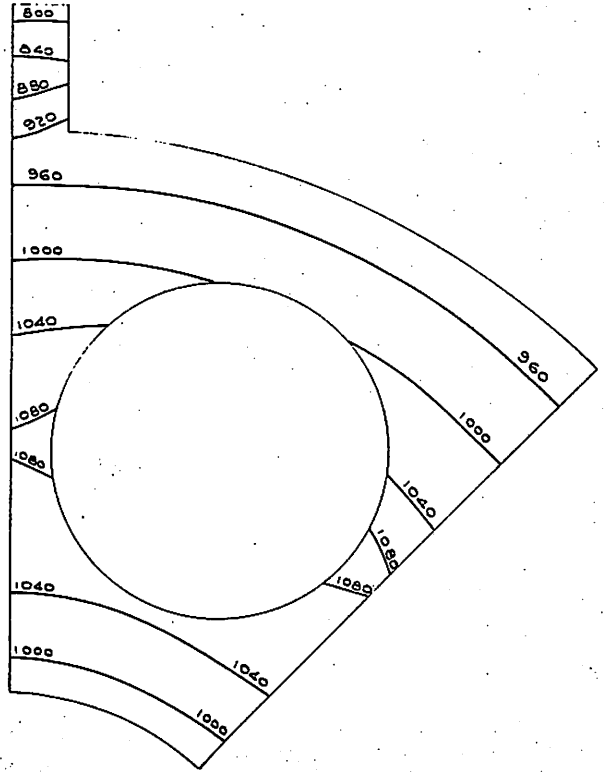

Fig. 3 Temperature Distribution (^{o}C)

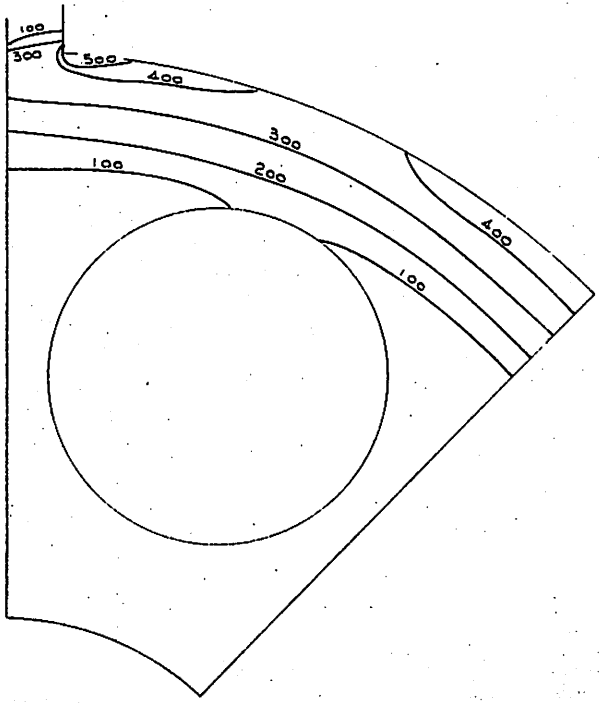

Fig. 4 Maximum Principal Stress in xy Plane at Time Zero (N/cm^2)

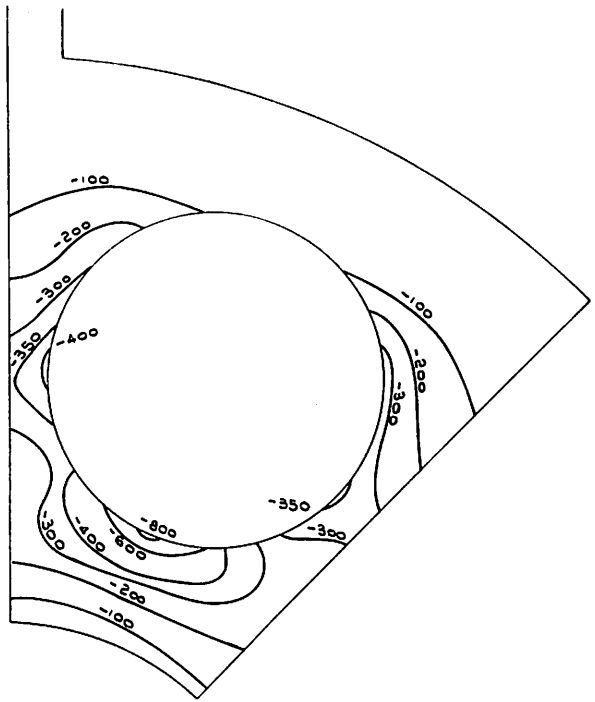

Fig. 5 Minimum Principal Stress in xy Plane at Time Zero (N/cm^2)

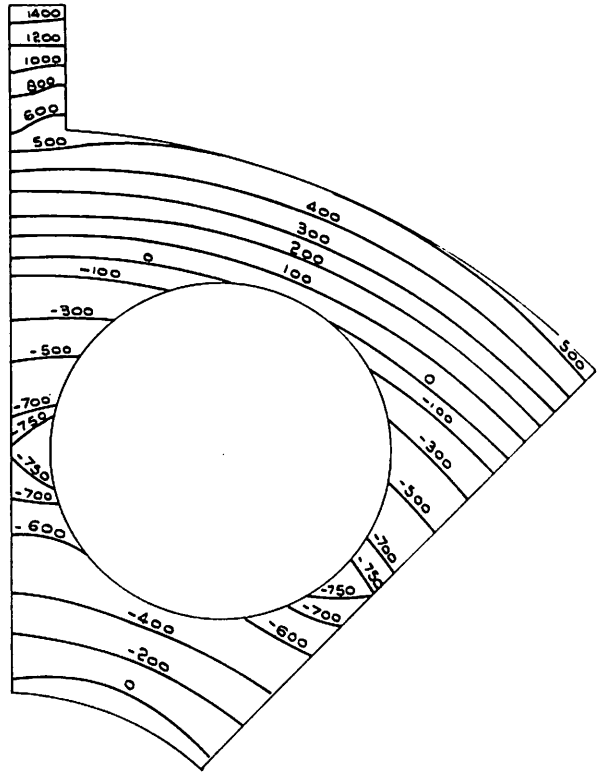

Fig. 6 Stress in Axial Direction at Time Zero (N/cm^2)

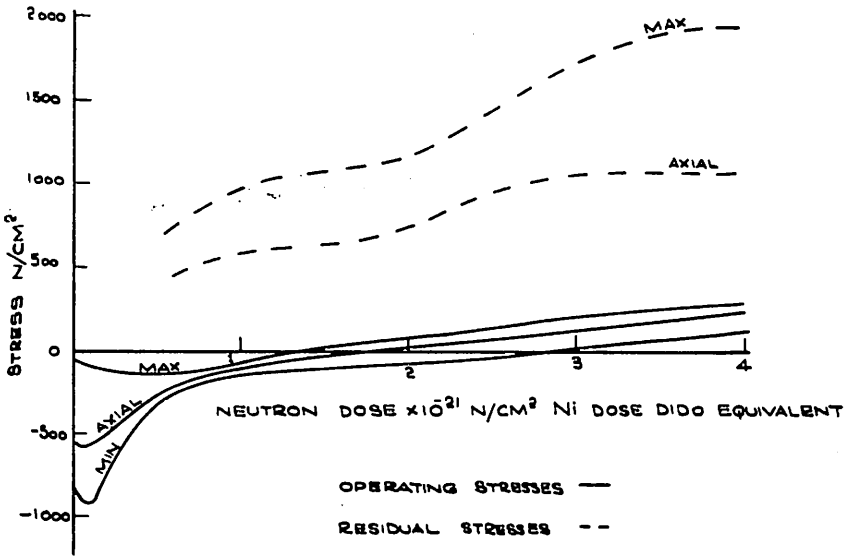

Fig. 7 Variation with Time of Principal Stresses on Element 488 - Reactor at Power and Shut Down

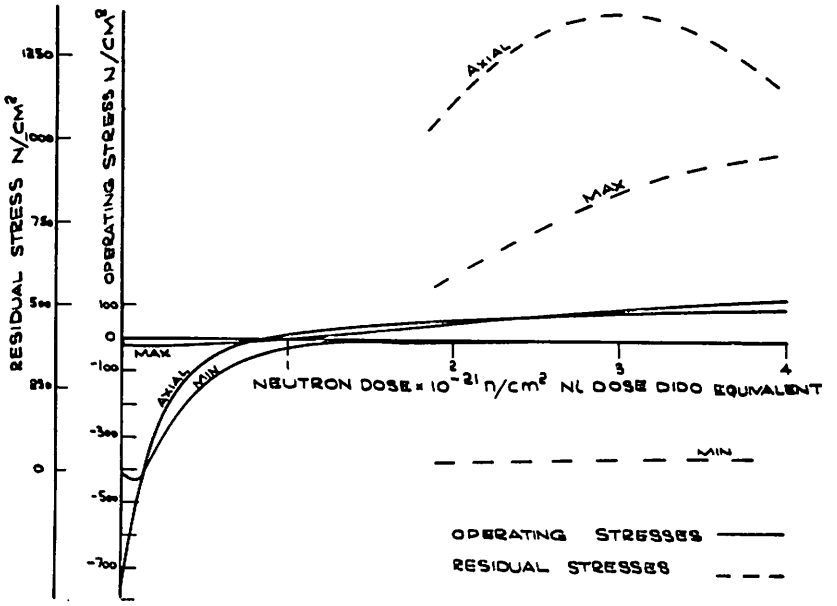

Fig. 8 Variation with time of Principal Stresses on Element 401 - Reactor at Power and Shut Down

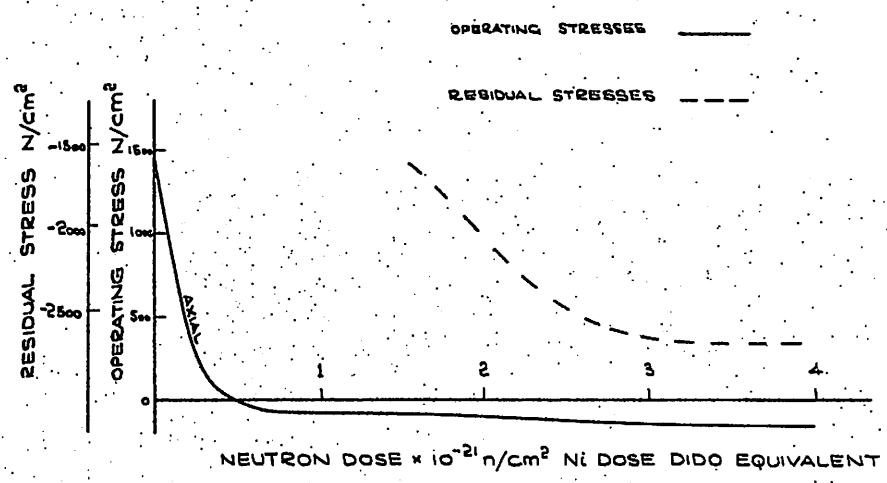

Fig. 9 Variation with Time of Axial Stress on Element 4 - Reactor at Power and Shut Down.

DISCUSSION

Q A. DONEA, JRC Ispra, Italy

Did you develop any algorithm to "optimize" the choice of the successive time steps in your creep solution ?

A A. JEZERNIK, U. K.

We have not developed any algorithm to optimize the choice of the successive time steps, but we believe that a partial iteration of creep strains (3-10 iterations) at each time step will be useful and compatible with a larger time (dose) step. It is thought that such a creep iteration together with a large time step will be especially desirable for the time-dependent calculations where the changes of the elastic constants with time are considered, since in this case the computer calculations are considerably more time-consuming than in the case where the constants are assumed to be constant in time.

Q F. C. WEILER, U. S. A.

The axial stresses in the locating rib seemed extremely large (1400 N/cm^2). Do these stresses exceed the maximum allowable stresses for your graphite material ?

A A. JEZERNIK, U. K.

The axial stresses in the locating rib are very high since we have assumed that the pin is restricted from bowing. Since some bowing of the pin can be expected the real stresses will probably have considerably lower values. We have considered and studied the amount of possible bowing of the pin but the results are not yet available.

C F. C. WEILER, U. S. A.

Yes, I agree, that since these ribs are only used to center the fuel element, then some engineering judgment can be used to eliminate this condition by redesign.